Integrated multiscale analysis reveals complex gender-specific changes in lymphocytes of smokers

Anne-Cécile Ribou, Florence Riera, Fabienne Durand, Laurent Henry

Environmental Toxicology and Pharmacology 111 (2024) 104566

Contents lists available at ScienceDirect

Environmental Toxicology and Pharmacology

journal homepage: www.elsevier.com/locate/etap

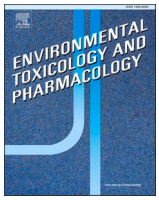

Integrated multiscale analysis reveals complex gender-specific changes in lymphocytes of smokers

Anne-Cécile Ribou [a,b,*], Florence Riera [a,b], Fabienne Durand [a,b], Laurent Henry [c,d]

[a] Espace-Dev, Univ. Perpignan Via Domitia, Bat. B, 52 av. Paul Alduy, Perpignan 66860, France
[b] Espace-Dev, UMR 228, Univ. Montpellier, UPVD, IRD, Montpellier, France
[c] IBMM CNRS UMR5247, Univ, Montpellier, France
[d] Laboratoire d'Histologie-Embryologie-Cytogénétique, Faculté de Médecine Montpelier-Nîmes, Nimes, France

ARTICLE INFO

Edited by Dr. M.D. Coleman

Keywords:
Tobacco toxicity
Cell imaging
Flow cytometry
Circulating lymphocyte
Discriminant analysis, Gender

ABSTRACT

Environmental stressors induce specific physiological responses that can be measured in the blood, notably by morphological changes in lymphocytes. Tobacco being the best-known stress in terms of its impact on health, we studied the physiological properties of peripheral blood lymphocytes in a population of 33 healthy non-smokers and smokers. Proteasome amount, mitochondria energy levels, changes in membrane properties and cell and nuclear size were analyzed to obtain 28 parameters from two fluorescence-based techniques: flow cytometry and cell imaging. The results showed that none of the parameters alone identified gender and smoking status, but that statistical analysis of these parameters, whether or not combined with a third set of data, hematological data, can. Statistical analysis of selected parameters clearly discriminates between male and female samples, as well as smokers and non-smokers. Effects of tobacco smoke pollutants are more pronounced in female smokers than in other groups.

1. Introduction

Circulating lymphocytes are a highly organized living system, easily sampled from blood and maintained in culture while preserving their properties. Analyzed in various inflammatory diseases, they are a prime indicator of the aggression of environmental factors on the human organism (Orakpoghenor et al., 2019). Tobacco is responsible for millions of annual deaths and chronic diseases, many of which occur prematurely. Although considered a behavioral risk, it can be seen as an environmental factor detrimental to human health, as tobacco smoke contains over 4000 compounds, a mixture of toxic compounds such as arsenic, for example, with synergistic effects (Talhout et al., 2011). The effects of smoking on health are numerous, attacking lung, throat and mouth, but also the heart and vessels, inducing cardio-vascular disease, among the major risks (Qiu et al., 2017; Ribassin-Majed and Hill, 2015). Worldwide, the tobacco control strategy encourages research into the consequences of smoking and interventions to reduce cigarette consumption (Reitsma et al., 2017; Shibuya, 2003).

Smoking habits have been shown to influence cellular parameters in blood when studying direct blood counts (Malenica et al., 2017; Pedersen et al., 2019). The detection of changes in lymphocyte properties has been studied on lymphocytes subpopulations (Piaggeschi et al., 2021; Schaberg et al., 1997), in relation to immune systems (Dahdah et al., 2022; Martos et al., 2020; Qiu et al., 2017; Stämpfli and Anderson, 2009), chromosomal damages (Farkas et al., 2021), and DNA methylation (Su et al., 2016) with sometimes contradictory conclusions. Other biomarkers can be evaluated to detect physiological changes in lymphocytes. Among these, cell imaging microscopy can be used to study the morphology and cellular functions of individual cells. It allows to analyze hundreds of cells, but rarely rare events. Data acquisition is rapid, and live cells can be labeled with multiple probes. Using triple labeling (R123, NR, Ho342) (Lautier et al., 1993; Rocchi et al., 2000; Savatier et al., 2012), we can obtain information on mitochondrial energy levels, changes in membrane properties and cell and nuclear sizes. In addition, using flow cytometry, we analyzed the proteasome subunit content (Baz et al., 1997; Henry et al., 1997) with specific fluorescent tags for 10 proteasome subunits. The amount of proteasome in several thousand cells can thus be analyzed. Last but not least, hematological parameters obtained from complete blood count (CBC) can be easily added to the above information (Gunawardena et al., 2016).

* Corresponding author at: Espace-Dev, Univ. Perpignan Via Domitia, Bat. B, 52 av. Paul Alduy, Perpignan 66860, France.
E-mail addresses: ribou@univ-perp.fr (A.-C. Ribou), florence.riera@univ-perp.fr (F. Riera), fabienne.durand@univ-perp.fr (F. Durand), laurent.henry@umontpellier.fr (L. Henry).

https://doi.org/10.1016/j.etap.2024.104566
Received 17 May 2024; Received in revised form 4 September 2024; Accepted 7 September 2024
Available online 10 September 2024

In a first attempt to investigate differences between normal lymphocytes and lymphocytes under environmental stress, we studied the effect of tobacco on a human population sample comprising men and women. 41 parameters were obtained from CBC and isolated lymphocyte analyses. Parameters were compared between smokers and non-smokers, taking gender into account, to identify the most relevant parameters to distinguish gender and smoking status. Based on the selected parameters, a multiparametric analysis (discriminant factor analysis, DFA) was used. DFA clearly distinguishes smokers from non-smokers and women from men. Circulating lymphocytes appear to be an interesting reservoir of information, enabling a quantitative approach to the study of the effect of environmental stresses. The aim of this study was to determine whether the morphology, physiology, and proteasome content of lymphocytes could be powerful and sufficient indicators in the study of environmental stress.

2. Material and methods

2.1. Patients

Healthy blood donors were prospectively recruited by the Etablissement Français du Sang in the city of Perpignan (Occitanie, France) between April 1997 and April 1998. This organization was responsible for blood collection and all participants completed a medical

Table 1
Characteristics of smoking on blood count parameters and lymphocyte proteasomal, functional and morphological contents, stratified by gender.

	Cases			**Controls**		
	Total	Male **SM**	Female **SF**	Total	Male **nSM**	Female **nSF**
Sample characteristic[a]	(n=15)	(n=11)	(n=4)	(n=18)	(n=10)	(n=8)
Nicotine exposure mg/day (min-max)	(36–72)	(36–72)	(36–72)	0	0	0
Demographics						
Male (n (%))	11 (73 %)	-	-	10 (55 %)	-	-
Age, years	43.0 (7)	42.0 (7)	43.3 (6)	46.4 (11)	47.2 (10)	45.5 (13)
Hemogram parameters						
WBC $10^3/mm^3$	8 (3)	8 (3)	9 (2)	5 (1)	5(1)	5.7 (0.7)
LYMP $10^2/mm^3$	28 (6)	29 (6)	25 (1.5)	33 (7)	36 (4)	30 (8)
MONO $10^2/mm^3$	5.5 (1)	5.5 (1.5)	5.5 (0.4)	6 (2)	6 (2)	6 (1)
GR $10^2/mm^3$	67 (6)	66 (7)	70 (1)	60 (7)	57 (4)	64 (8)
RBC $10^6/mm^3$	4.6 (0.3)	4.6 (0.3)	4.6 (0.4)	4.4 (0.3)	4.6 (0.3)	4.1 (0.2)
Hb g/dl	14.5 (1.4)	15 (1)	13.1 (0.5)	14 (1)	14.4 (0.9)	12.7 (0.4)
Hct %	42 (3)	42 (3)	42 (4)	39 (4)	41 (3)	36.5 (1.5)
MCV fL	91 (4)	90 (4)	92 (4)	89 (4)	90 (5)	88 (4)
MCH pg	31.5 (2.6)	32 (2)	29 (3)	31.2 (1.5)	31 (2)	31 (1)
MCHC g/dl	35 (3)	35.9 (0.7)	33 (5)	35 (2)	35 (2)	34.9 (0.9)
RDW %	13.3 (0.8)	13.2 (0.9)	13.4 (0.6)	12.5 (0.6)	12.3 (0.4)	12.6 (0.9)
PLT $10^3/mm^3$ added	231 (50)	232 (50)	230 (50)	212 (30)	205 (25)	221 (35)
PLR % = PLT/LYMP	87 (30)	85 (30)	92 (20)	67 (20)	57 (10)	80 (30)
Isolated lymphocytes						
Proteasome parameters						
Number of treated cells	2900 (500)	3100 (500)	2500 (150)	3200 (100)	3400 (750)	2983 (850)
MFIp21	76 (35)	72 (35)	86 (40)	130 (110)	125 (120)	136 (110)
MFIp23	270 (220)	290 (250)	220 (140)	420 (350)	460 (430)	370 (230)
MFIp25	60 (35)	60 (35)	58 (35)	74 (50)	77 (60)	71 (30)
MFIp27	74 (45)	67 (40)	93 (50)	87 (50)	82 (65)	94 (40)
MFIp29	66 (35)	61 (30)	80 (40)	87 (50)	84 (60)	90 (45)
MFIp3033	60 (30)	60 (30)	62 (35)	89 (70)	93 (90)	84 (50)
MFIp31	65 (30)	60 (25)	79 (35)	92 (60)	88 (70)	97 (40)
%cell+p21	49 (20)	48 (20)	54 (20)	50 (15)	51 (20)	48 (10)
%cell+p23	57 (15)	56 (20)	59 (10)	54 (15)	56 (20)	52 (9)
%cell+p25	38 (15)	39 (20)	36 (4)	42 (15)	45 (20)	38 (10)
%cell+p27	50 (20)	49 (20)	54 (10)	49 (15)	50 (20)	49 (15)
%cell+p29	47 (20)	47 (20)	47 (8)	47 (20)	51 (20)	41 (15)
%cell+p3033	46 (20)	47 (20)	46 (20)	46 (10)	47 (15)	46 (10)
%cell+31	46 (20)	47 (20)	42 (9)	47 (15)	48 (20)	43 (10)
Functional information						
Number of treated cells (n)	180 (80)	150 (60)	280 (40)	170 (60)	180 (75)	160 (35)
$FI-1_{max}$ NR	16,500 (7100)	16,700 (8000)	15,900 (4100)	15,300 (4000)	15,300 (3100)	15,300 (4900)
MFI NR	19,700 (7000)	20,000 (7500)	18,600 (4300)	20,000 (6000)	18,600 (2700)	22,000 (9000)
SD NR	8800 (2500)	9500 (2600)	7000 (1300)	10,000 (5000)	8600 (3400)	12,400 (6600)
$FI-1_{max}$ R123	1550 (800)	1500 (750)	1700 (850)	1400 (500)	1500 (650)	1200 (360)
MFI R123	1900 (800)	1900 (800)	2000 (980)	2000 (1000)	2000 (1000)	1900 (1000)
SD R123	1100 (700)	1200 (700)	900 (300)	1400 (1000)	1300 (1000)	1500 (1000)
Morphological parameters						
$Cell-1_{max}$	230 (30)	230 (35)	220 (25)	230 (20)	230 (10)	230 (25)
Mean Cell	250 (30)	250 (40)	230 (15)	250 (25)	250 (25)	250 (25)
SD Cell	71 (40)	79 (40)	49 (6)	76 (40)	67 (30)	87 (50)
% Cell>350	0.1 (0.1)	0.1 (0.1)	0.04 (0.03)	0.10 (0.098)	0.09 (0.08)	0.11 (0.08)
$Cell/Nuc-1_{max}$	1.33 (0.08)	1.32 (0.09)	1.375 (0.001)	1.4 (0.1)	1.4 (0.15)	1.4 (0.1)
Mean Cell/Nuc	1.5 (0.3)	1.5 (0.3)	1.49 (0.06)	1.5 (0.2)	1.5 (0.2)	1.5 (0.1)
SD Cell/Nuc	0.6 (0.3)	0.6 (0.4)	0.4 (0.015)	0.5 (0.2)	0.5 (0.2)	0.5 (0.25)
% Cell/Nuc>3	0.05 (0.08)	0.06 (0.09)	0.009 (0.002)	0.03 (0.04)	0.03 (0.04)	0.04 (0.05)

Abbreviations: SD, standard-deviation; WBC, white blood cell number, all other abbreviations in Table 2.
[a] Variable distribution are reported as mean (SD) unless otherwise specified.

questionnaire on arrival, were informed by an information letter and signed a written consent in accordance with the Declaration of Helsinki [34]. The donors were living in an agricultural area (south of France). The health status of the donors was checked and the sample population was free of alcohol drinkers and had normal transaminase levels (SGPT and SGOT) excluding a possible effect of hepatic toxic chemicals. The smoking criterion was a consumption of 20–40 cigarettes per day (nicotine exposure approximately 36–72 mg/day), Table 1. Approval for this study was obtained from the local ethics committee at the time of patient recruitment, and has recently been updated (CHU Nîmes, ref: 23.08.08).

2.2. Blood analysis

Three distinct experiments were performed on each blood sample. A complete blood count (CBC) was performed immediately after blood collection. Following the lymphocyte isolation, the cells were separated into two pools, one for flow cytometric analysis of proteasome parameters, and the other intended for fluorescence cell imaging to acquire morphological parameters and functional information regarding each individual cell.

2.2.1. Hematological parameters

The CBC provided numeration of white blood cells (WBC), lymphocytes (LYMP), monocytes (MONO), granulocytes (GR) and platelets (PLT), as well as measurements on erythrocyte variables, such as the number of red blood cell (RBC), hemoglobin (Hb), hematocrit (Hct), mean corpuscular volume (MCV), mean cell Hb (MCH), mean cell Hb concentration (MCHC), red cell distribution width (RDW). The platelet/lymphocyte ratio (PLR) was calculated as an inflammatory marker (Tulgar et al., 2016). Raw data and boxplots are presented in supplementary material (Table S1, Fig. S1A).

2.2.2. Isolation of lymphocytes from peripheral blood

Lymphocytes were isolated by Ficoll-gradient centrifugation from venous blood in non-heparinized tubes. Cells were then incubated in a serum-free culture medium (X-VIVO 10, Bio-Whittaker) at 1 ×106 cells/ml in 25 cm2 culture flask. Lymphocytes cultures were left in an incubator at 37°C in a humid atmosphere with 5 % CO2, and the lymphocyte population was studied within 24 hours. After 4 days more than 99 % of lymphocytes still excluded Trypan Blue.

2.2.3. Proteasome parameters

Seven monoclonal antibodies from mouse ascite (distributed by Organon Teknica, Turnhoot, Belgium) directed against human core proteasome alpha subunits were used (De Sa et al., 1988). Clones anti-p23, p25 (clone A 7A11), p27 (IB5), p29 (GD6), p30–33 and p31 (AA4) respectively recognize proteasomal alpha-subunit PSMA7 (De Conto et al., 2000), PSMA3, PSMA6, PSMA9, PSMA2 and PSMA8, while clone anti-p21 recognizes protein p21, known as prosome-like particle (Akhayat et al., 1987). Protocol of flow cytometry is detailed in (Henry et al., 1996). Shortly concerning antibodies: dilution 1/50 and incubation time 30 min. Flow cytometry and multiple staining of fixed and permeabilized (70 % ethanol) cells enabled us to study intra- and extracellular proteasomes (Machiels et al., 1995). This protocol makes it possible to fix the cells and preserve their structure, while permeabilizing them sufficiently for the antibodies to penetrate the cell and reach their target. 3100 ± 700 cells per donor were analyzed after exclusion of debris of size and morphology for at least three experiments (Table S2, Fig. S1B).

2.2.4. Morphological parameters and functional information

Cell morphology and physiology was analyzed using fluorescence imaging. Cells were labelled with three fluorescent probes (i.e. triple labeling). Hoechst 33342 (Ho342) is a vital nucleus-specific fluorescent dye (Bainbridge and Macey, 1983; Fuchs et al., 2023; Lahmy et al., 1993). Mitochondria-specific Rhodamine 123 (R123) (Darzynkiewicz et al., 1981; Johnson et al., 1980) is described as a probe of mitochondrial energy status (Johnson et al., 1980; Lahmy et al., 1993), and Nile Red (NR) is a fluorescent probe trapped in the plasma membrane (Mukherjee et al., 2007; Sackett and Wolff, 1987) that allows clear delineation of the cell contour and observation of changes in membrane properties (Canitrot et al., 1993). The triple labelling protocol (cell labelling, numerical image analysis and recorded parameters) has already been described in detail (Savatier et al., 2003) and can be consulted in the supplementary materials. The analysis was performed on 180 ± 70 cells per donor (Table S3, Fig. S1C).

2.3. Statistical analysis

Multifactorial analysis and statistical tests were performed using XLStat software from Addinsoft®, Paris, France (version 2021–4–1 and 2022–2–2 BASIC+). Univariable analyses of the 41 parameters were performed using tests adapted to small sample sizes and therefore less sensitive to data non-normality. To analyze the parameters one-by-one, the mean, median and standard deviation was calculated for six sub-populations (Table 1) and represented in box plots (Fig. S1). Variations between sub-populations was assessed in pairs (Fig. 1 and Table S4) by calculating (i) the percentage variation using the equation % var = (x-y)/mean(x,y) with x represents the parameters for smokers or men, and y the parameters for non-smokers or women, and (ii) the adjusted p-value calculated using the Benjamini & Hochberg correction. Ridge, Lasso, and the combined regressions were performed in order to identify and select the most relevant parameters for the analysis, by minimizing overfitting and improving the predictive power of the model.

Discriminant factors analysis (DFA) is a statistical method for multivariate data that distinguishes between 'x' predefined sample groups. XLStat's DFA method aims to categorize a set of n donors (i.e. training population) into x distinct groups using a set of predictor variables (p, where $p < n$). This is achieved by creating of discriminant functions, representing linear combinations of p variables that best discriminate the x pre-defined groups. The results are displayed on x-1 factorial axes (factor space). In the software, two models are available using quadratic or linear discriminant functions. In our case, only the linear model was available because of the small number of donors, n. In this study we obtained the blood of 33 donors, n=33, and parameters was measured or calculated for three set of experimental data (i.e. p = 41 variables). It was therefore necessary to reduce the number of variables to a number less than n. However, this was not necessary when testing univariate or bivariate analyses, using one or two of the three experimental sets, as the total number of parameters for bivariate analyses ($\leq$28) remains lower than the number of donors.

The donor population was divided in groups before the DFA. Four groups (x = 4) separating smokers from non-smokers and females from male. Three groups excluding female smokers due to the scarcity of this group (only four female smokers agreed to take part in the study). But also, two groups to assess smoking habit (smokers and non-smokers) or gender influence (male and female), separately. When only two groups are to be predicted, DFA is close to logistic regression, but present the interest to provide graphs. All DFA's were also performed with and without the "fixed class weight" option to test the relevance of this option. This option provides a compensation when heterogeneity in the group size is observed. Not surprisingly, using this option ameliorates all DFAs from four group (i.e. including the four female smokers), but not DFAs from three groups.

The software facilitates actions such as reclassifying misclassified donors into groups and running statistical tests, including the Wilks' Mahalonobis inter-group distance test. It can be used to check on graphs (i) whether the groups assigned to donors are distinct on factorial axes, (ii) to identify the parameters characterizing the groups on a correlation circle. The results are presented as confusion matrices for the training

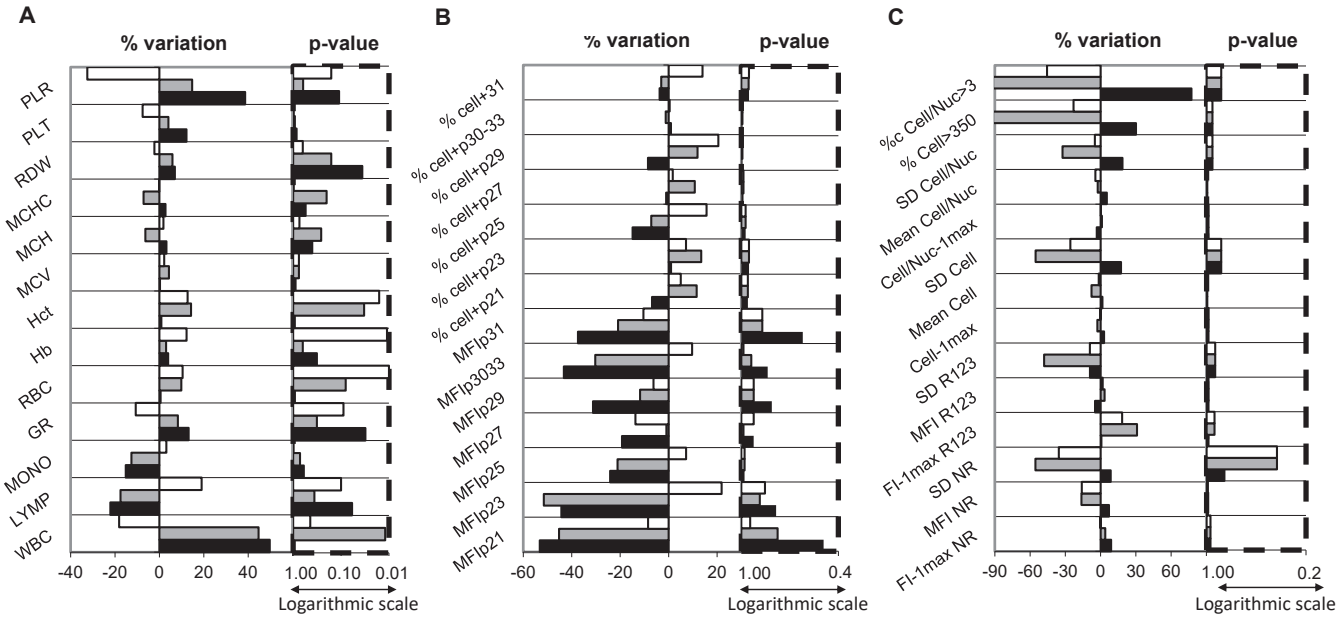

Fig. 1. Inter-population variations for the 41 parameters. Parameters analyzed individually across three pairs: male smokers versus male non-smokers (black), female smokers versus female non-smokers (grey), and male versus female non-smokers (white). See Table S4 for the other two pairs. (A) Hematogram data information (13 parameters), (B) Proteasome analysis lymphocyte by flow cytometry (14 parameters), (C) Quantitative cellular imaging of lymphocyte (14 parameters of cell morphology and physiology). Left: Percentage variation of the mean, with positive variation indicating increase in the parameter. Right: Adjusted p-value (Benjamini & Hochberg) on a logarithmic scale.

population, expressed as percentages that indicate the training accuracy of the classification, with 100 % meaning no misclassification of donors. Since the prediction can be overly optimistic, the software offers cross validation as a measure of the model's performance. This involves performing calculations by removing one donor at a time of the training population and then predicting the group for that donor (leave-one-out method). Expressed as a percentage, a validation accuracy of 100 % means that the model has correctly classified all the donors in the validation sets.

3. Results

Thirty-three healthy blood donors (21 men and 12 women) agreed to take part in the study. Their ages were 44.9 ± 9 and 44.7 ± 9 years respectively. They all lived in an agricultural area with little industrial activity and a generously ventilated environment in the south of France. Our sample included 4 female smokers and 12 male smokers.

3.1. Blood analysis

The blood parameters of each donor were analyzed using three set of experimental data: (i) complete blood count, (ii) proteasome analysis by lymphocyte flow cytometry and (iii) lymphocyte cell analysis by fluorescence imaging, yielding 41 variables for study (Table 2). Raw data are presented in supplementary material (Tables S1–S3 for hematological, proteasome and cell imaging data, respectively), along with the box plots separated by gender and smoking status (Fig. S1). The amount of proteasomal antigen was calculated and presented as mean fluorescence intensity per cell (MFI) and percentage of positive cells (% cell+) marked by antibodies. Note that the average intensity before correction by cell number is very high for the detection of anti-p23 (1650 ± 190) with a ratio to irrelevant antibody (total mouse immunoglobins) of 18. The p25, p29 et p30–33 subunits (506 ± 29, 370 ± 13, and 490 ± 20, respectively) are well detected with a ratio between 4 and 6. In contrast, detection of p27 and p31 is poor (184 ± 13, and 165 ± 5, respectively) with a ratio below 2. After triple labeling of live lymphocytes, we obtained probe intensity (total, mean and standard error for Ho342, R123 and NR), parameters more related to physiological cell properties, and the number of illuminated pixel (cell and nucleus area and perimeter, shape factors), related to morphology. Next, lymphocyte population properties were analyzed using histograms of cell population distributions for each of the parameters, and the parameter was selected when the distribution differed between groups. In addition to the mean of the total fluorescence intensity (MTI), we presented the fluorescence intensity of the first peak of the distribution (FI-1_{max}) and the standard deviation (SD) of the heterogeneous lymphocyte population.

3.2. Analyses of the variation of the 41 parameters

Means and standard deviations are presented in Table 1 for six subpopulations (controls and smokers as a total population then separated by gender). To examine variations according to smoking habit, gender or both, five cases were evaluated in pairs (smokers vs. non-smokers in the total population and separated by gender, and men vs. women separated by smoking habit). Percentage variations between pairs and adjusted p-values (Table S4 for the five pairs, Fig. 1 for three selected pairs) were calculated for all the 41 parameters. Very few variations are significant (adjusted p-value less than 0.05) and only for CBC data (e.g. WBC). It is difficult, if not impossible, to obtain a trend from these hematological analyses. This is clearer for lymphocyte data: smoking induces a change in parameters in the same direction for proteasome-related parameters for men and women, but in an opposite direction for morphological and physiological parameters.

3.3. DFA analyses to differentiate gender or smoking habit

The three sets of experimental data were tested using univariate or bivariate analyses to differentiate between gender (Fig. 2, top) or smoking habit (Fig. 2, bottom), with discriminant factor analysis (DFA). Confusion matrices shows 100 % training accuracy in separating groups by gender, but validation accuracy ranging from 46 % to 69 %. No effect of age was observed, but a 64-years-old woman (donor 16) was grouped

Table 2
List of 41 parameters and their abbreviations. 14 morphological and physiological parameters obtained by fluorescence cell imaging on lymphocytes, 14 proteasomal parameters obtained by flow cytometry on lymphocytes and 13 hematological parameters from CBC examination.

no.	Abbreviation	Meaning of the parameter
	Cell imaging on lymphocytes	
1	**FI−1$_{max}$ NR**	Nil Red: Max Fluorescence Intensity of the 1st peak of the distribution
2	**MFI NR**	Nil Red: Mean of Fluorescence Intensity
3	**SD NR**	Nil Red: Standard Deviation
4	**FI−1$_{max}$ R123**	R123: Max Fluorescence Intensity of the 1st peak of the distribution
5	**MFI R123**	R123: Mean Fluorescence Intensity
6	**SD R123**	R123: Standard Deviation
7	**Cell−1$_{max}$**	Cell Area: Max of the 1st peak of the distribution
8	**Mean Cell**	Cell Area: Mean of the pixel inside NR staining
9	**SD Cell**	Cell Area: Standard Deviation
10	**Cell/ Nuc−1$_{max}$**	Ratio Cell Area/Nucleus Area: Max of the 1st peak of the distribution
11	**Mean Cell/ Nuc**	Ratio Cell Area/Nucleus Area: Mean
12	**SD Cell/Nuc**	Ratio Cell Area/Nucleus Area:: Standard Deviation
13	**%c Cell>350**	% size of lymphocytes > 350 pixels
14	**%c Cell/ Nuc>3**	% ratio Cell Area/Nucleus Area > 3
	Proteasome parameters for lymphocytes	
15	**MFIp21**	Proteasome 21 K: Mean Fluorescence Intensity
16	**MFIp23**	Proteasome 23 K: Mean Fluorescence Intensity
17	**MFIp25**	Proteasome 25 K: Mean Fluorescence Intensity
18	**MFIp27**	Proteasome 27 K: Mean Fluorescence Intensity
19	**MFIp29**	Proteasome 29 K: Mean Fluorescence Intensity
20	**MFIp30–33**	Proteasome 30–33 K: Mean Fluorescence Intensity
21	**MFIp31**	Proteasome 31 K: Mean Fluorescence Intensity by cell
22	**%cell+p21**	% positive cells proteasome 21 K
23	**%cell+p23**	% positive cells proteasome 23 K
24	**%cell+p25**	% positive cells proteasome 25 K
25	**%cell+p27**	% positive cells proteasome 27 K
26	**%cell+p29**	% positive cells proteasome 29 K
27	**%cell+p30–33**	% positive cells proteasome 30–33 K
28	**%cell+31**	% positive cells proteasome 31 K
	Hemological parameters	
29	**WBC**	White blood cell number
30	**LYMP**	Lymphocyte number
31	**MONO**	Monocyte number
32	**GR**	Granulocyte number
33	**RBC**	Red blood cell number
34	**Hb**	Hemoglobin
35	**Hct**	Hematocrit
36	**MCV**	Mean corpuscular volume
37	**MCH**	Mean cell Hb
38	**MCHC**	Mean cell Hb concentration
39	**RDW**	RCB distribution width
40	**PLT**	Platelet number
41	**PLR**	Platelet-Lymphocyte ratio

close to the males when using hematogram data alone or combined with proteasome data. Neither proteasome analysis nor cell imaging analysis could distinguish between gender or smoking status (training accuracy was less than 86 %) (data not shown). Only the combination of proteasome/hematogram data distinguish smoking status (Fig. 2, bottom). Adjusting for the low number of female smokers using the "fixed class weight" option slightly improves separation in the CBC data, but has no effect on the other analyses.

3.4. DFA analyses to differentiate gender and smoking habit

In a DFA, we classified donors into four groups based on smoking status and gender, using univariate or bivariate analyses (Fig. 3). For bivariate analyses, training accuracy was 100 %, but validation accuracy was low (20 %, 26 % and 30 %, for A, B and C, respectively). In the bivariate analyses that combined CBC data (Fig. 3, B and C), the F3 axis was needed to distinguished males, though training accuracy remains at

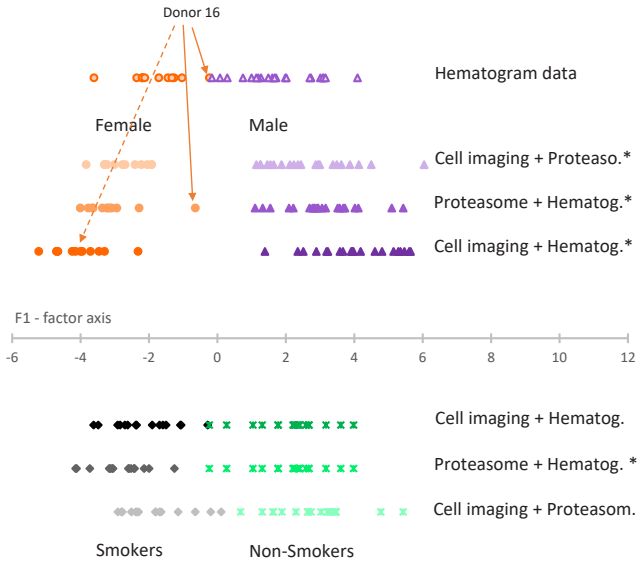

Fig. 2. Classification by DFA with the donors divided in two groups. Top: Subgroups by sex. Bottom: Subgroups by smoking habit. The three set of experimental data: quantitative lymphocytes cells imaging (p = 14), lymphocyte proteasome analysis by flow cytometry (p = 14) and hematogram data information (p = 13), were taken one at a time (univariate analysis) or two at a time (bivariate analysis). All DFAs presented are run using "fixed class weight" option. The asterisk means that the confusion matrices for the training population have a training accuracy of 100 %. Validation accuracy, from top to bottom, is 80 %, 46 %, 60 %, 69 % for gender and 48 %, 63 % and 48 % for smoking habit.

100 %. None of the univariable analyses could differentiate between the four groups, with hematological data (Fig. 3 D) achieving the best training accuracy (89 %) and 54 % validation accuracy. Removing female smokers slightly improved performance, with validation accuracy rising to 17 %, 31 % and 41 % (Fig. S3).

3.5. Can the selection of informative parameters improve the performance of the discriminant analyses?

To perform DFA with the parameters from the three experimental data sets, we needed to reduce the number of parameters to fewer than 33. We selected parameters (see Table 3) based on the following criteria: (i) pairwise variations between sub-populations greater than 12, (ii) proximity to the DFA correlation circle with coordinates greater than 0.3 on the F1 and/or F2 axes, indicating high information content in univariate analyses (iii) identification by Ridge, Lasso and the combination (elastic net) regressions from the 41 parameters. For the first two statistical analyses, DFA successfully separated donors into three or four groups with 100 % training accuracy (Fig. 4), but validation accuracy was around 50 %. The parameters selected by Ridge/Lasso regressions resulted in the lowest training accuracy (< 92 %) but high validation accuracy (60–70 %). To improve validation accuracy beyond 50 % while maintaining training accuracy at 100 %, we tried various strategies, including statistical clustering of the parameters (hierarchical classification and K-mean tests), but these did not yield clear results. Only four parameters from lymphocyte image analysis formed a distinct cluster. We then excluded and reintegrated parameters one-by-one, finding that increasing the number of parameters improved separation but often reduced validation accuracy when the added parameters provided no additional information. Using the final model with selected parameters (Table 2, last column), DFA confirmed the existence of four groups (Fig. 5 A) and three groups (Fig. 5 B) with 100 % training accuracy and validation accuracies of 81 % and 79 %, respectively. In the four-group analysis, cross-validation suggest that eight male donors

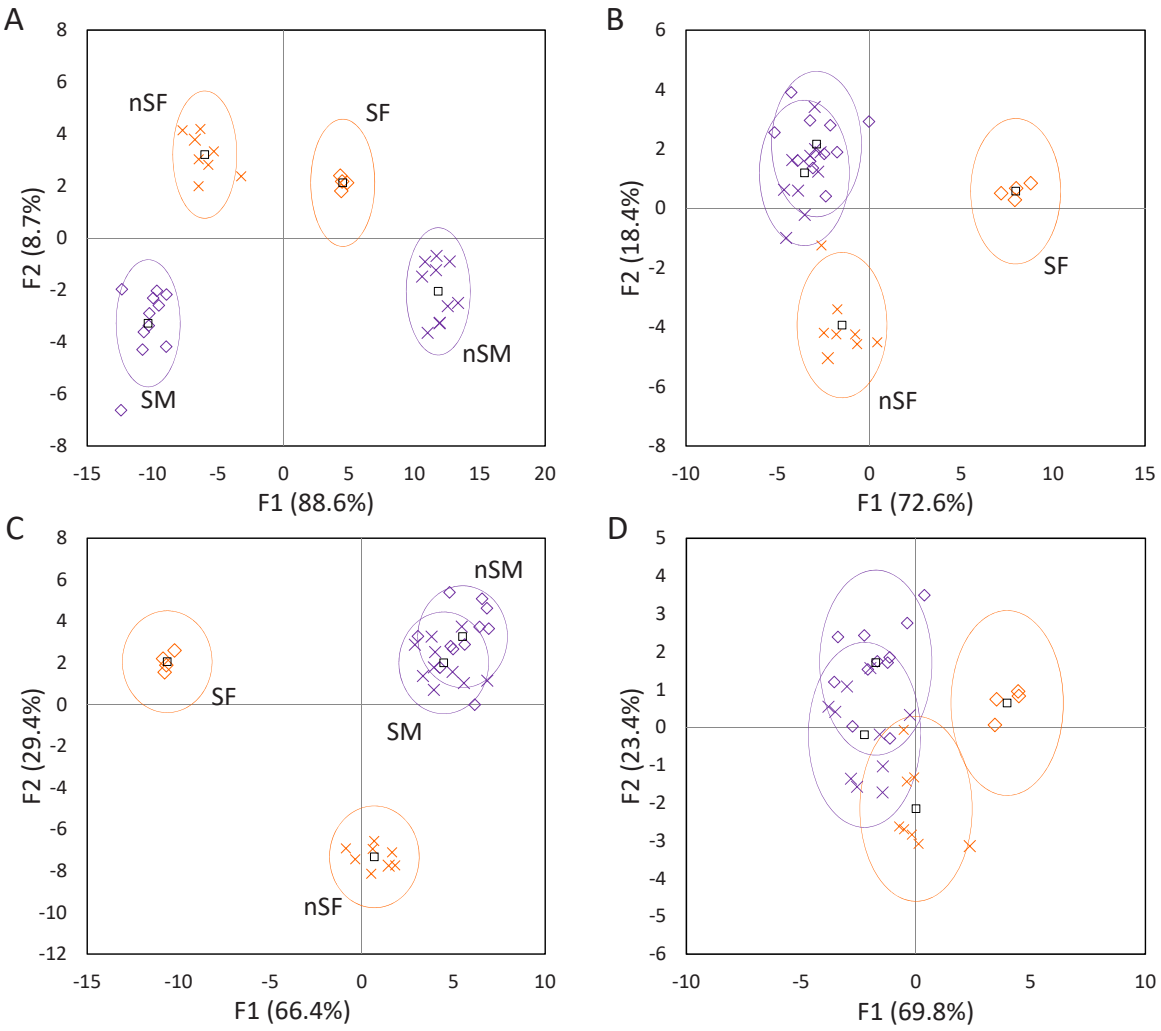

Fig. 3. Classification by DFA with the donors separated in four groups using univariate or bivariate analyses. Projection of the donors on the first two axes (F1 and F2) with confidence circles. Correlation circles provided in supplementary material (Fig. S2). SM: smoking male, SF: smoking female, nSM: non-smoking male, nSF: non-smoking female. (A) Lymphocyte-based analyses (Proteasome and imaging) (p = 28), (B) Proteasome and CBC data (p = 27), (C) Lymphocyte imaging and CBC data (p = 27), (D) CBC data only (p = 13). Statistical analyses were performed on 33 donors; analyses excluding female smokers (three groups) provided in supplementary material (Fig. S3).

(four smokers and four non-smokers) might be classified differently based on smoking status. In the three-group analysis (excluding female smokers), six donors might have been reassigned: two male smokers to the non-smokers group, two male non-smokers to the smoker groups and two female non-smokers to the male non-smokers group.

4. Discussion

Analyzing each parameter individually showed that some varied little or not at all due to gender or smoking habit. Some parameters, like RDW, showed minimal variation but had high adjusted p-value, while others, like MONO, showed the opposite. There was no clear relationship between high variation and a low p-value. For each experiment, we looked for parameters that best reflect smoking habits and also distinguish men from women. Smoking was more closely associated with WCB and PLR, which increased with smoking and showed significant variation and acceptable adjusted p-values. Indeed, elevate WCB is often consider a non-specific predictor of poor health conditions and a good candidate for assessing smoking (Kabat et al., 2017; Smith et al., 2003). More recently, increased PLR, typically related to environmental stress, has been linked to smoking (Pujani et al., 2021; Tulgar et al., 2016). However, those two parameters were not selected for inclusion in the final model because they did not significantly help distinguish between groups and could reduce the overall classification accuracy. LYMP and MONO decrease with smoking in both men and women, and although some p-value were initially below 0.05, they became non-significant after adjustment. Gender differences were also observed, with higher LYMP and Hb levels and lower WBC levels in both smokers and non-smokers. However, it is challenging, if not impossible, to identify a clear trend from these individual analyses. If a parameter shows a distinct pattern in one group, such as Hct in non-smoking women, it can skew the results for sex, gender, and the overall population

The mean fluorescence intensity (MFI) per cell of all tested proteasomes (p21, p23, p25, p29, p30–33 and p31), differed between smokers and non-smokers, with tag intensity – indicating the amount of proteasomes - decreasing in smokers. This aligns with existing literature, which reported that cigarette smoke inhibits proteasome activity both *in vitro*, *in vivo* (Van Rijt et al., 2012). However, no significant difference was observed in our study. Furthermore, while the MFI of all proteasomes decreased in both male and female smokers, no consistent gender-related trend was observed. Although sex hormones are known to affect proteasome function, with studies suggesting higher proteasome activity in female mice tissues (Jenkins et al., 2020), activity and quantity are not directly comparable. The percentage of positively

Table 3
Summary of informative parameters selected from the three experimental datasets. The selected parameters were used in DFA with the donors divided in four groups and three groups (without female smokers). The results are presented as training accuracy and validation accuracy (in brackets) as percentages. Column 1: Inter-groups mean variation greater than 12. Column 2: Parameters closest to the DFA correlation circle, with coordinates greater than 0.3 in the univariate analyses (Fig. S2). Column 3: Parameters identified by Elastic Net regression (see Table S5 for more details). Column 4: Parameters yielding the best validation accuracy for DFA in four groups. Column 5: Parameters giving the best validation accuracy for DFA in three groups.

Mean variation		Correlation Circle*		Elastic Net Regression		final reduction		final reduction	
4 groups 100 % (42 %)	3 groups 100 % (26 %)	4 groups 100 % (49 %)	3 groups 100 % (38 %)	4 groups 92 % (71 %)	3 groups 93 % (62 %)	4 groups **100 % (81 %)**	3 groups 95 % (65 %)	4 groups 100 % (71 %)	3 groups **100 % (79 %)**
MFI NR									
SD NR		SD NR		SD NR				SD NR	
FI−1_{max} R123									
						MFI R123			
SD R123						(80 % without)			
				Cell/Nuc−1_{max}					
SD Cell		SD Cell				SD Cell		SD Cell	
SD Cell/Nuc		SD Cell/Nuc (F2)				SD Cell/Nuc		SD Cell/Nuc	
% Cell>350		% Cell>350				% Cell>350		% Cell>350	
% Cell/Nuc>3		% Cell/Nuc>3				% Cell/Nuc>3		% Cell/Nuc>3	
MFIp21		MFIp21 (F2)							
MFIp23		MFIp23 (F2)							
MFIp25									
MFIp27		MFIp27 (F2)				MFIp27		MFIp27	
MFIp29		MFIp29 (F2)				MFIp29		MFIp29	
MFIp3033		MFIp3033 (F2)				MFIp3033		MFIp3033	
MFIp31		MFIp31 (F2)		MFIp31		MFIp31		MFIp31	
%cell+p21									
%cell+p23									
%cell+p25									
%cell+p29									
%cell+31									
WBC		WBC							
LYMP		LYMP						LYMP	
MONO									
		GR		GR		GR			
		RBC (F2)		RBC		RBC		RBC	
Hb		Hb		Hb		Hb			
Hct		Hct (F2)				Hct		Hct	
MCV						MCV			
MCH		MCH				MCH		MCH	
		MCHC							
		RDW		RDW		RDW		RDW	
PLR		PLR							

* close to F2 axis if indicated between brackets, close to F1 axis if not.

labelled cells showed little variation, particularly between male smokers and non-smokers, again these differences were not significant. Overall, the labelling by our antibody pool tended to decrease under stress conditions, which is consistent with expectations.

Lymphocyte morphology and physiology showed a greater difference between smokers and non-smokers in women, with opposite patterns often observed in smoking men. However, similar to the proteasome data, none of the p-values, whether adjusted or not, were significant. Cell morphology parameters such as SD Cell, SD Cell/Nuc, and the percentage of 'abnormal cells' increased in male smokers but surprisingly decreased in female smokers. The number of large lymphocytes (% Sc $>$ 350) and those with small nuclei (% Sc/Sn $>$ 3) is extremely low in female smokers. This finding should be tempered by the fact that only four female smokers participated in the study. Functional parameters coming from membrane and mitochondrial markers (NR and R123, respectively), also showed varying tends depending on gender, resulting in no overall variation. Although mitochondrial labelling (FI-1_{max} R123) increased in both male and female smokers, it was extremely low in female non-smokers, but was not selected in the final model.

In summary, unlike proteasomal and most CBC measurements, cellular imaging provides parameters that vary differently according to sex and smoking habits. If men and women are not analyzed separately, general trends such as decreased proteasomes and increased leukocytes will be observed, but this will mask the specific effects of smoking on lymphocyte morphology and physiology. This highlights the importance of considering gender when studying the effects of smoking.

Given the lack of significant variations in individual lymphocyte parameters, analyzing the experiments as a whole was crucial. The three experimental datasets were tested separately and in pairs to differentiate between gender or smoking habit. Of the analyses, only the CBC data differentiated gender, but not smoking habit. Interestingly, all pairwise analyses successfully distinguished men from women, while only one combination -proteasome combined with hematogram data- effectively predicted smoking habits. The other two combinations misclassified one or two donors, different each time. Despite this, a trend emerged. To further investigate, the same procedure was used to separate the donors into four groups based on gender and smoking habits using univariate or bivariate analyses. Only pairwise analyses successfully distinguished all four groups, showing a clear separation between men and women, with one of the factorial axes capturing this distinction when proteasome and imaging data were combined. However, no factorial axis contained information on smoking habits, likely due to cell imaging data revealing predominantly opposite patterns for male and female smokers. Cross-validation remains low, with more than half of the donors potentially reassigned to a different group. By selecting more informative parameters, with the greatest variation or with highest information (as defined by the position on correlation circle), gender and/or smoking habit separated more clearly on the F1/F2 factor space, eliminating the inversion of positions for male and female smokers. Together, these

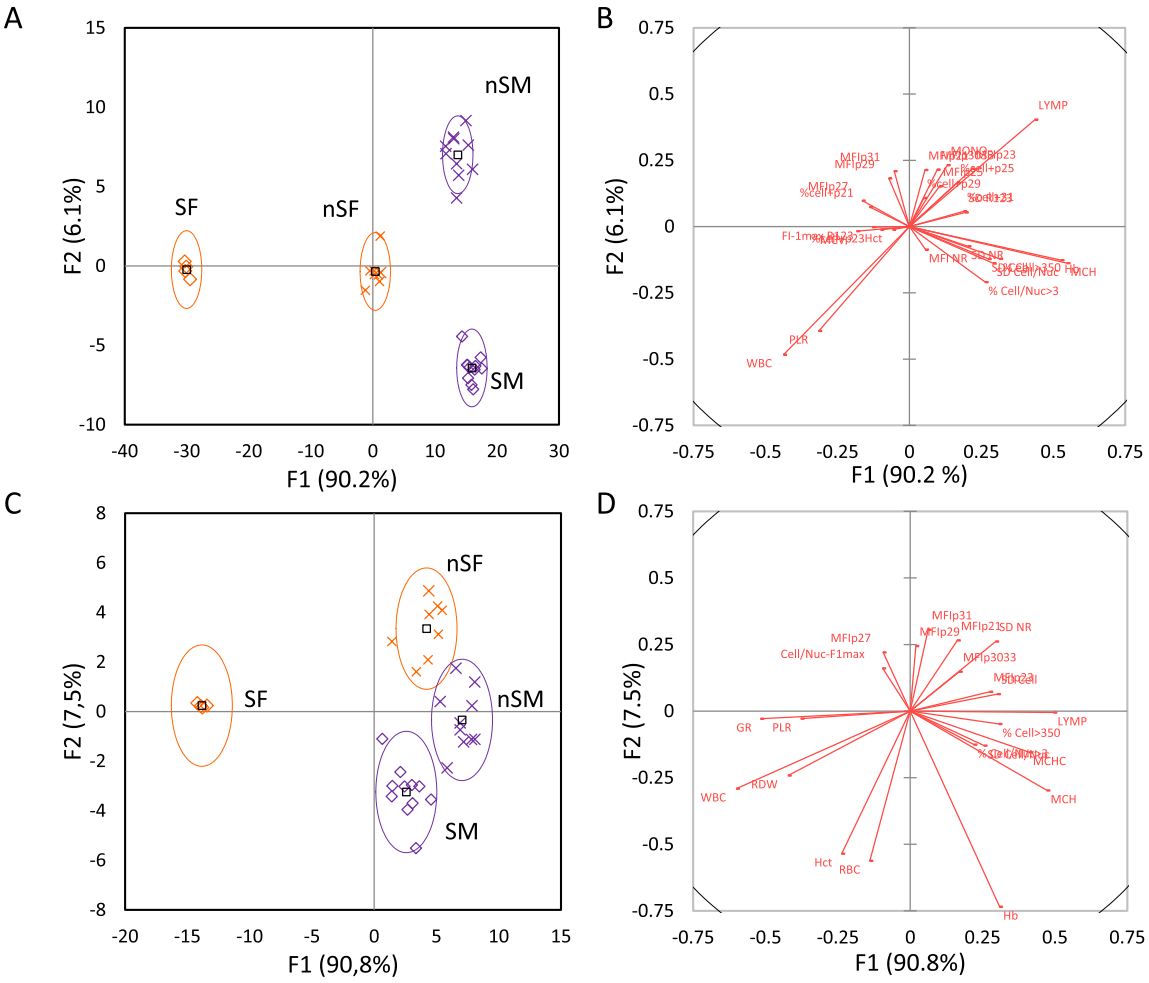

Fig. 4. DFA classification into four groups using a reduced number of parameters. Parameters selected based on the following criteria: (A, B) Inter-groups mean variation greater than 12 %. (C, D) Proximity to the DFA correlation circle with coordinates greater than 0.3 on the F1 and/or F2 axes in the three univariable DFA analyses. (A, C) Projection of donors onto the factor space (F1 and F2) with confidence circles; (B, D) Correlation circle showing the projection of parameters on the factor space. A zoomed in view is provided to distinguish between parameters. In these two DFAs, all the donors were correctly separated (training accuracy 100 %). Validation accuracy: (A) 42 % (26 % for three groups), (C) 49 % (38 % for three groups).

selections improved validation accuracy up to 50 %. The parameters selected by Ridge, Lasso and Elastic Net regressions are listed in Table S5. All these parameters were already identified and included in the final model, except for Cell/Nuc-F1$_{max}$. They are necessary but not sufficient to achieve a clear separation into four groups. Here again, it would be interesting to test what happens with a larger number of donors. An additional manual selection of a dozen parameters allows us to better distribute information on gender and smoking habit between the two axes, with a visual separation of smokers and gender on the F1/F2 factors axes. In addition, this method finally achieves validation accuracy of 80 %. Interestingly, although no statistical effect of age was observed, donors 16 and 12 aged 64 and 63 respectively, were among the donors reassigned during cross validation.

This study identified several key parameters that appear consistently in the different statistical analysis. Parameters related to cell morphology, derived from cell imaging, were retained. While proteasome intensity parameters were retained, no parameters related to the percentage of marked cells were included. Most of the parameters retained were derived from CBC, even though parameters such as GR, RBC and RDW did not show high inter-population variation or significant p-values. Contrary to expectations, the addition of parameters (SD NR and LYM) improved separation when smokers were excluded from the dataset.

5. Conclusions

In this study, we combined a small number of donors, in particular female smokers, with a statistical method, ADF, which requires a smaller number of experimental parameters than the number of donors. Despite this limitation, the process of reducing the number of parameters allowed us to identity key parameters and highlight the relevance of lymphocytic cells. A larger population would likely provide a deeper understanding of these parameters and improve the selection process needed to confidently separate the four groups. Integrating the three experimental datasets with multiparametric statistics demonstrated that the effect of smoking on blood tests and lymphocytes is significant, especially in women, emphasizing the importance of considering gender when studying the effect of smoking. This work also underscores the potential of fluorescence imaging in revealing the wealth of lymphocytes properties. This approach could be valuable for studying the effect of tobacco, classifying control individuals, and conducting more detailed analyses, such as assessing consumption levels, the impact of smoking cessation, alternatives to cigarettes, or nicotine substitutes. Additionally, it could be highly useful for monitoring environmental stressors or endocrine disruptors.

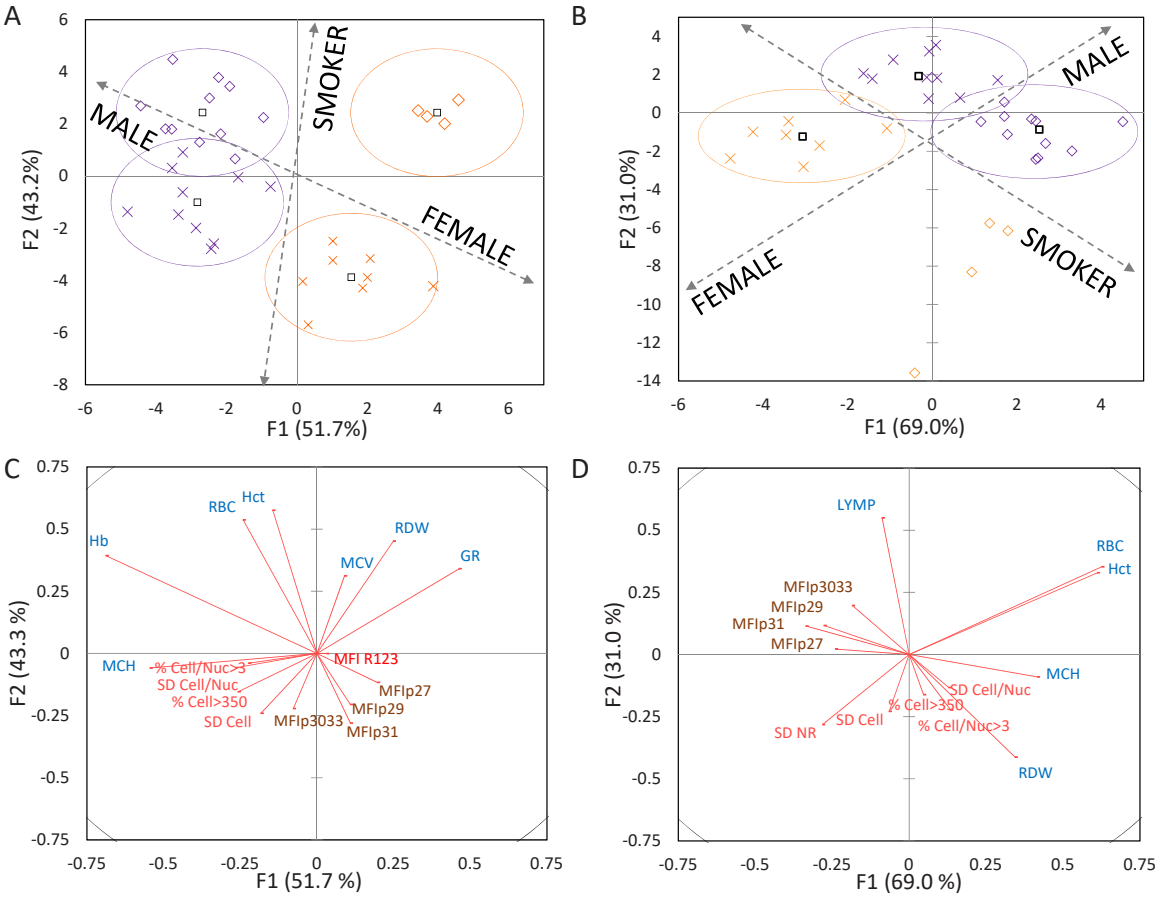

Fig. 5. Final classification by DFA. Donors were separated in four groups (A C) and three groups (B, D) (n = 33 and n = 29 by removing female smokers, respectively). Sixteen and fourteen selected parameters were included in the analysis (Table 3). (A, B): Projection of donors on the first two axes (F1 and F2), with confidence circles. (C, D): Correlation circle, zoomed in to distinguished between parameters. DFA was run using the "fixed class weight" option for the four-group analysis but not for the three-group analysis. In Figure B, female smokers were reintroduced as variables to be predicted. SM: smoking male, SF: smoking female, nSM: non-smoking male, nSF: non-smoking female. In all four DFAs, donors were correctly separated (training accuracy = 100 %), with validation accuracy of 81 % (A) and 79 % (B).

CRediT authorship contribution statement

Fabienne Durand: Writing – review & editing, Validation. **Laurent Henry:** Writing – review & editing, Investigation, Formal analysis. **Anne-Cecile Ribou:** Writing – original draft, Visualization, Supervision, Methodology, Investigation, Formal analysis, Conceptualization. **Florence Riera:** Writing – review & editing, Validation, Formal analysis.

Funding

This research did not receive any specific grant from funding agencies in the public, commercial, or not-for-profit sectors.

Declaration of Competing Interest

The authors declare that they have no known competing financial interests or personal relationships that could have appeared to influence the work reported in this paper.

Data availability

data have been added to the supplementary material

Acknowledgements

We would like to thank or deceased colleagues Jean-Marie Salmon and Jean Vigo for having started this work, they strongly contributed to statistical analyses, and our retired colleague Jean-Paul Bureau for initiating and supervising proteasome research. Judith Pesco for recording part of the cellular fluorescence image during her doctorate (2000, "Study by fluorescence imaging and multiparametric analysis of the variability of circulating lymphocyte populations").

Appendix A. Supporting information

Supplementary data associated with this article can be found in the online version at doi:10.1016/j.etap.2024.104566.

References

Akhayat, O., Infante, A.A., Infante, D., Martins de SA, C., Grossi de SA, M.-F., Scherrer, K., 1987. A new type of prosome-like particle, composed of small cytoplasmic RNA and multimers of a 21-kDa protein, inhibits protein synthesis in vitro. Eur. J. Biochem. 170, 23–33. https://doi.org/10.1111/j.1432-1033.1987.tb13663.x.

Bainbridge, D.R., Macey, M.M., 1983. Hoechst 33258: a fluorescent nuclear counterstain suitable for double-labelling immunofluorescence. J. Immunol. Methods 62, 193–195. https://doi.org/10.1016/0022-1759(83)90246-6.

Baz, A., Henry, L., Chateau, M.-T., Scherrer, K., Bureau, J.P., 1997. Subcellular distribution and profiles of prosomes (proteasomes-MCP) during differentiation of human lymphoblastic cell line. Leuk. Res. 21, 1061–1070. https://doi.org/10.1016/S0145-2126(97)00091-X.

Canitrot, Y., Lautier, D., Lahmy, S., Vigo, J., Viallet, P., Salmon, J.M., 1993. Nile red labeling of single living cells for contour delineation to quantify and evaluate the

distribution of rhodamine 123 with fluorescence image cytometry. J. Histochem. Cytochem. 41, 1785–1793. https://doi.org/10.1177/41.12.8245427.
Dahdah, A., Jaggers, R.M., Sreejit, G., Johnson, J., Kanuri, B., Murphy, A.J., Nagareddy, P.R., 2022. Immunological insights into cigarette smoking-induced cardiovascular disease risk. Cells 11, 3190. https://doi.org/10.3390/cells11203190.
Darzynkiewicz, Z., Staiano-Coico, L., Melamed, M.R., 1981. Increased mitochondrial uptake of rhodamine 123 during lymphocyte stimulation. Proc. Natl. Acad. Sci. USA 78, 2383–2387. https://doi.org/10.1073/pnas.78.4.2383.
De Conto, F.D., Pilotti, E., Razin, S.V., Ferraglia, F., Géraud, G., Arcangeletti, C., Scherrer, K., 2000. In mouse myoblasts nuclear prosomes are associated with the nuclear matrix and accumulate preferentially in the perinucleolar areas. J. Cell Sci. 113, 2399–2407. https://doi.org/10.1242/jcs.113.13.2399.
De Sa, M.F.G., De Sa, C.M., Harper, F., Coux, O., Akhayat, O., Pal, J.K., Florentin, Y., Scherrer, K., 1988. Cytolocalization of prosomes as a function of differentiation. J. Cell Sci. 89, 151–165. https://doi.org/10.1242/jcs.89.2.151.
Farkas, G., Kocsis, Z.S., Székely, G., Dobozi, M., Kenessey, I., Polgár, C., Jurányi, Z., 2021. Smoking, chromosomal aberrations, and cancer incidence in healthy subjects. Mutat. Res./Genet. Toxicol. Environ. Mutagen. 867, 503373 https://doi.org/10.1016/j.mrgentox.2021.503373.
Fuchs, H., Jahn, K., Hu, X., Meister, R., Binter, M., Framme, C., 2023. Breaking a dogma: high-throughput live-cell imaging in real-time with hoechst 33342. Adv. Healthc. Mater. N./a, 2300230. https://doi.org/10.1002/adhm.202300230.
Gunawardena, D., Jayaweera, S., Madhubhashini, G., Lokumarakkala, D.D., Senanayake, S.J., 2016. Reliability of parameters of complete blood count with different storage conditions. J. Clin. Lab Anal. 31, e22042 https://doi.org/10.1002/jcla.22042.
Henry, L., Baz, A., Château, M.T., Scherrer, K., Bureau, J.P., 1996. Changes in the amount and distribution of prosomal subunits during the differentiation of U937 myeloid cells: high expression of p23K. Cell Prolif. 29, 589–607. https://doi.org/10.1111/j.1365-2184.1996.tb00974.x.
Henry, L., Baz, A., Château, M.T., Caravano, R., Scherrer, K., Bureau, J.P., 1997. Proteasome (prosome) subunit variations during the differentiation of myeloid U937 cells. Anal. Cell Pathol. 15, 131–144. https://doi.org/10.1155/1997/869747.
Johnson, L.V., Walsh, M.L., Chen, L.B., 1980. Localization of mitochondria in living cells with rhodamine 123. Proc. Natl. Acad. Sci. USA 77, 990–994. https://doi.org/10.1073/pnas.77.2.990.
Kabat, G.C., Kim, M.Y., Manson, J.E., Lessin, L., Lin, J., Wassertheil-Smoller, S., Rohan, T. E., 2017. White blood cell count and total and cause-specific mortality in the women's health initiative. Am. J. Epidemiol. 186, 63–72. https://doi.org/10.1093/aje/kww226.
Lahmy, S., Lautier, D., Canitrot, Y., Laurent, G., Salmon, J.M., 1993. Staining with hoechst-33342 and rhodamine-123 - an attempt to detect multidrug-resistant phenotype cells in leukemia. Leuk. Res. 17, 1021–1029. https://doi.org/10.1016/0145-2126(93)90158-h.
Lautier, D., Lahmy, S., Canitrot, Y., Vigo, J., Viallet, P., Salmon, J.M., 1993. Detection of human leukemia cells with multidrug-resistance phenotype using multilabeling with fluorescent dyes. Anticancer Res. 13, 1557–1563.
Machiels, B.M., Henfling, M.E., Broers, J.L., Hendil, K.B., Ramaekers, F.C., 1995. Changes in immunocytochemical detectability of proteasome epitopes depending on cell growth and fixation conditions of lung cancer cell lines. Eur. J. Cell Biol. 66, 282–292.
Malenica, M., Prnjavorac, B., Bego, T., Dujic, T., Semiz, S., Skrbo, S., Gusic, A., Hadzic, A., Causevic, A., 2017. Effect of cigarette smoking on haematological parameters in healthy population. Med Arch. 71, 132–136. https://doi.org/10.5455/medarh.2017.71.132-136.
Martos, S.N., Campbell, M.R., Lozoya, O.A., Wang, X., Bennett, B.D., Thompson, I.J.B., Wan, M., Pittman, G.S., Bell, D.A., 2020. Single-cell analyses identify dysfunctional CD16+ CD8 T cells in smokers. Cell Rep. Med. 1, 100054 https://doi.org/10.1016/j.xcrm.2020.100054.
Mukherjee, S., Raghuraman, H., Chattopadhyay, A., 2007. Membrane localization and dynamics of Nile Red: effect of cholesterol. Biochim. Et. Biophys. Acta (BBA) - Biomembr. 1768, 59–66. https://doi.org/10.1016/j.bbamem.2006.07.010.
Orakpoghenor, O., Avazi, D.O., Markus, T.P., Olaolu, O.S., 2019. Lymphocytes: a brief review. Sci. J. Immunol. Immunother. 3, 004–008.
Pedersen, K.M., Çolak, Y., Ellervik, C., Hasselbalch, H.C., Bojesen, S.E., Nordestgaard, B. G., 2019. Smoking and increased white and red blood cells. Arterioscler. Thromb. Vasc. Biol. 39, 965–977. https://doi.org/10.1161/ATVBAHA.118.312338.
Piaggeschi, G., Rolla, S., Rossi, N., Brusa, D., Naccarati, A., Couvreur, S., Spector, T.D., Roederer, M., Mangino, M., Cordero, F., Falchi, M., Visconti, A., 2021. Immune trait shifts in association with tobacco smoking: a study in healthy women. Front Immunol. 12, 637974 https://doi.org/10.3389/fimmu.2021.637974.
Pujani, M., Chauhan, V., Singh, K., Rastogi, S., Agarwal, C., Gera, K., 2021. The effect and correlation of smoking with platelet indices, neutrophil lymphocyte ratio and platelet lymphocyte ratio. Hematol. Transfus. Cell Ther. 43, 424–429. https://doi.org/10.1016/j.htct.2020.07.006.
Qiu, F., Liang, C.-L., Liu, H., Zeng, Y.-Q., Hou, S., Huang, S., Lai, X., Dai, Z., 2017. Impacts of cigarette smoking on immune responsiveness: Up and down or upside down? Oncotarget 8, 268–284. https://doi.org/10.18632/oncotarget.13613.
Reitsma, M.B., et al., 2017. Smoking prevalence and attributable disease burden in 195 countries and territories, 1990–2015: a systematic analysis from the Global Burden of Disease Study 2015. Lancet 389, 1885–1906. https://doi.org/10.1016/S0140-6736(17)30819-X.
Ribassin-Majed, L., Hill, C., 2015. Trends in tobacco-attributable mortality in France. Eur. J. Public Health 25, 824–828. https://doi.org/10.1093/eurpub/ckv078.
Rocchi, E., Vigo, J., Viallet, P., Bonnard, I., Salmon, J.M., 2000. Multiwavelength videomicrofluorometric study of cytotoxic effects of a marine peptide, Didemnin B, on normal and MDR resistant CCRF-CEM cell lines. Anticancer Res. 20, 987–996.
Sackett, D.L., Wolff, J., 1987. Nile red as a polarity-sensitive fluorescent probe of hydrophobic protein surfaces. Anal. Biochem. 167, 228–234. https://doi.org/10.1016/0003-2697(87)90157-6.
Savatier, J., Rharass, T., Canal, C., Gbankoto, A., Vigo, J., Salmon, J.-M., Ribou, A.-C., 2012. Adriamycin dose and time effects on cell cycle, cell death, and reactive oxygen species generation in leukaemia cells. Leuk. Res. 36, 791–798. https://doi.org/10.1016/j.leukres.2012.02.017.
Savatier, J., Vigo, J., Salmon, J.M., 2003. Monitoring cell cycle distributions in living cells by videomicrofluorometry and discriminant factorial analysis. Cytom. Part A 56, 8–14. https://doi.org/10.1002/cyto.a.10080.
Schaberg, T., Theilacker, C., Nitschke, O.T., Lode, H., 1997. Lymphocyte subsets in peripheral blood and smoking habits. Lung 175, 387–394. https://doi.org/10.1007/pl00007585.
Shibuya, K., 2003. WHO Framework Convention on Tobacco Control: development of an evidence based global public health treaty. BMJ 327, 154–157. https://doi.org/10.1136/bmj.327.7407.154.
Smith, M.R., Kinmonth, A.-L., Luben, R.N., Bingham, S., Day, N.E., Wareham, N.J., Welch, A., Khaw, K.-T., 2003. Smoking status and differential white cell count in men and women in the EPIC-Norfolk population. Atherosclerosis 169, 331–337. https://doi.org/10.1016/s0021-9150(03)00200-4.
Stämpfli, M.R., Anderson, G.P., 2009. How cigarette smoke skews immune responses to promote infection, lung disease and cancer. Nat. Rev. Immunol. 9, 377–384. https://doi.org/10.1038/nri2530.
Su, D., Wang, X., Campbell, M.R., Porter, D.K., Pittman, G.S., Bennett, B.D., Wan, M., Englert, N.A., Crowl, C.L., Gimple, R.N., Adamski, K.N., Huang, Z., Murphy, S.K., Bell, D.A., 2016. Distinct epigenetic effects of tobacco smoking in whole blood and among leukocyte subtypes. PLoS One 11, e0166486. https://doi.org/10.1371/journal.pone.0166486.
Talhout, R., Schulz, T., Florek, E., Van Benthem, J., Wester, P., Opperhuizen, A., 2011. Hazardous compounds in tobacco smoke. Int. J. Environ. Res. Public Health 8, 613–628. https://doi.org/10.3390/ijerph8020613.
Tulgar, Y.K., Cakar, S., Tulgar, S., Dalkilic, O., Cakiroglu, B., Uyanik, B.S., 2016. The effect of smoking on neutrophil/lymphocyte and platelet/lymphocyte ratio and platelet ındices: a retrospective study. Eur. Rev. Med. Pharmacol. Sci. 20, 3112–3118.
Van Rijt, S.H., Keller, I.E., John, G., Kohse, K., Yildirim, A.Ö., Eickelberg, O., Meiners, S., 2012. Acute cigarette smoke exposure impairs proteasome function in the lung. Am J Physiol Lung Cell Mol Physiol. 303, L814–823. https://doi.org/10.1152/ajplung.00128.2012.